Hydrogen-Bonded PTCDA−Melamine Networks and Mixed Phases

J. C. Swarbrick,[†] B. L. Rogers,[†] N. R. Champness,[‡] and P. H. Beton*[,†]

Schools of Chemistry and Physics and Astronomy, University of Nottingham, University Park, Nottingham NG7 2RD, United Kingdom

Received: November 10, 2005; In Final Form: February 1, 2006

A stable hydrogen-bonding junction is formed between 3,4,9,10-perylene-3,4,9,10-tetracarboxylic-dianhydride (PTCDA) and 1,3,5-triazine-2,4,6-triamine (melamine). This bimolecular system was studied on the Ag−Si(111) $\sqrt{3} \times \sqrt{3}$R 30° surface at sub-monolayer coverage, and two distinct phases are observed. A hexagonal lattice is formed that is stabilized by hydrogen bonding between PTCDA and melamine. This phase, in which melamine acts as a 3-fold vertex, is a close analogue to the 3,4,9,10-perylene-3,4,9,10-tetracarboxylic-diimide−melamine network reported recently. To our knowledge this hydrogen-bonding junction has not been previously observed and might not be expected due to lone pair repulsion. However we confirm that this combination is stable using ab initio methods. In the second intermixed phase parallel rows of PTCDA molecules coexist with an array of melamine molecules, and we propose a model for this structure.

1. Introduction

The influence of hydrogen bonding on adsorbed supramolecular systems is currently of great interest[1,2] both for fundamental studies of interactions and in the formation of surface nanostructures. These systems can be investigated using scanning tunneling microscopy (STM) to directly observe molecular arrangements on a surface. Highlights of recent research include the formation of molecular arrays on surfaces stabilized by hydrogen bonds between dimers of carboxylic acid (O−H···O hydrogen bonds),[3,4] N−H···O carboxylic acid and nitrogen interactions,[5] C−H···O interactions,[6] and diimide[7] and dianhydride interactions.[8]

The use of two molecular species to form intermixed bimolecular arrangements offers enhanced control of molecular organization. For example, regular hexagonal arrays are formed by combining melamine and cyanuric acid to form junctions[9,10] stabilized by N−H···N hydrogen bonds. Bimolecular phases on surfaces have recently been studied using STM, with notable examples such as Cu−phthalocyanine and C_{60} on Cu(111) forming a commensurate ordered intermixed phase[11] and the coverage-dependent intermixed phases formed with chloro-[subphthalocyaninato]boron(III) (Sub(Pc)) and C_{60} on Ag(111).[12,13] Of particular relevance to this study is the formation of a supramolecular network by Theobald et al.[14,1] following the coadsorption of 3,4,9,10-perylene-3,4,9,10-tetracarboxylic-diimide (PTCDI) and 1,3,5-triazine-2,4,6-triamine (melamine) on the Ag−Si(111) $\sqrt{3} \times \sqrt{3}$R 30° surface. Here the interaction of PTCDI diimide groups with melamine diaminopyridine groups[9,10] gives rise to a stable nanopore template that was used to capture clusters of C_{60}[1] or C_{84}.[14]

In this study we investigate the formation of intermixed phases of 3,4,9,10-perylene-3,4,9,10-tetracarboxylic-dianhydride (PTCDA) (Figure 1a) and melamine (Figure 1b). PTCDA comprises a perylene core with anhydride groups on each end, and melamine has three amine groups bonded to a triazine ring. Deposition of PTCDA only on the Ag−Si(111) $\sqrt{3} \times \sqrt{3}$R 30° surface leads to the formation of three coexisting close-packed phases, which are described elsewhere.[8] Deposition of melamine on a sample with a sub-monolayer coverage of PTCDA induces the formation of two stable intermixed molecular phases, completely different from phases formed by PTCDA alone. A hexagonal network, similar to that observed by Theobald et al.,[1,14] is observed alongside a new double row structure, which consists of alternating double rows of PTCDA and melamine. Unlike many of the hydrogen-bonded junctions discussed above, anhydride−melamine hydrogen bonding has not previously been observed in related areas of chemistry. The hexagonal network phase is partly stabilized by the PTCDA anhydride groups interacting with two amine groups of the melamine via two N−H···O hydrogen bonds. In particular we note that this configuration is stable despite an expected repulsive interaction between the central dianhydride oxygen atom and the nitrogen atom in the melamine ring.

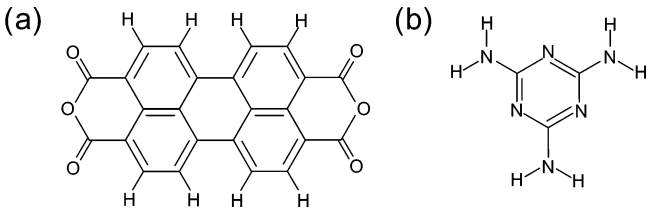

Figure 1. Molecules studied: (a) PTCDA, with a perylene core and dianhydride end groups, and (b) melamine, a triazine ring with three amine groups.

2. Experimental Methods

Images were acquired using a scanning tunneling microscope operating in constant current mode at room temperature in an ultrahigh vacuum (UHV) system (base pressure 1×10^{-10} Torr). Electrochemically etched tungsten tips, cleaned prior to use by electron beam heating, were used throughout. Atomically clean Si(111) was prepared by degassing a piece of p-type Si(111) wafer, then annealing to 1150 °C to form a (7 × 7) surface

* Author to whom correspondence should be addressed. E-mail: peter.beton@nottingham.ac.uk.
[†] School of Physics and Astronomy.
[‡] School of Chemistry.

10.1021/jp056517k CCC: $33.50
Published on Web 03/01/2006

reconstruction, which was characterized using STM. Silver was then deposited, while the sample was heated to 550°C, to form the hexagonal Ag−Si(111) $\sqrt{3} \times \sqrt{3}$R 30° reconstruction.[15] On this surface, all dangling bonds are saturated. Several organic molecules have previously been studied on this surface[1,7,8] and were found to diffuse readily over the surface at room temperature and form ordered arrays and islands mediated by intermolecular interactions.

The molecules were degassed thoroughly prior to deposition. PTCDA (99.9% pure, Sigma-Aldrich) was deposited at 330 °C for 15−20 min to achieve ~0.15 ML coverage. To investigate the PTCDA−melamine system, melamine (99% pure, Sigma-Aldrich) was subsequently sublimed from a home-built evaporator at 90°C for 15 min on top of the PTCDA-covered sample. The sample was held at room temperature during deposition, and no further annealing took place after the melamine deposition. The entire experiment was performed in the same three-chamber UHV system.

Experimental studies were supported by calculations performed using the SIESTA package.[16,17] The code performs calculations within the linear combination of atomic orbitals (LCAO) approximation using the self-consistent density functional theory (DFT). The generalized gradient approximation (GGA) was implemented using the Becke gradient exchange functional[18] and the modified Lee, Yang, and Parr correlation functional.[19] Core-corrected pseudo-potentials constructed according to the method described by Troullier and Martins were employed for all atoms.[20] Valence electrons were described by double-ζ basis sets with polarization functions. Calculations were performed using an energy shift, which defines the radius within which the atomic orbitals are strictly localized, of 0.001 Ry. Geometry optimization was performed using the conjugate gradient method with a convergence force tolerance of 0.01 eV $Å^{-1}$. The default convergence tolerance of 10^{-4} eV was employed for the self-consistent field (SCF) cycle at each stage of the optimization. Counterpoise corrections as described by Boys and Bernardi[21] were used to reduce the numerical error within the calculated interaction energies as a result of the well-known basis set superposition error (BSSE).

3. PTCDA and Melamine

Immediately after the deposition of PTCDA on the Ag−Si(111) $\sqrt{3} \times \sqrt{3}$R 30° surface, three close-packed phases are observed: a herringbone phase, a square phase, and a hexagonal structure. These are discussed in detail elsewhere.[8] Deposition of melamine onto these samples completely changes the surface morphology, suggesting the PTCDA phases, though stable enough to be imaged many times, are readily converted to a new phase by the addition of melamine on the surface. The introduction of C_{60} or adenine onto the surface, rather than melamine, does not change the PTCDA phases, and these molecules simply segregate into islands with no mixed molecular phases forming. Figure 2 shows the overall surface morphology, with PTCDA and melamine supramolecular structures covering the surface. In this image the bright features that are clearly resolved are PTCDA molecules. Two distinct phases are present in small regions (~20 nm across). The short rows with a width of two molecules constitute the double row phase. The other phase, which appears less abundantly, is the hexagonal network.

3.1. Hexagonal Networks. The PTCDA−melamine hexagonal network is shown in Figure 3. Each bright feature is a PTCDA molecule. The hexagonal networks were observed to have a maximum size of approximately 30 hexagonal units. The insert in Figure 3 shows intramolecular features resolved within the PTCDA molecules. Each molecule has two bright lobes with a darker contrast line along the center. As we have shown previously, this corresponds to the shape of the highest occupied molecular orbital (HOMO), calculated using DFT for an isolated molecule. The two lobes of the HOMO run along the long axis of the molecule (Figure 1 in ref 8). This intramolecular contrast allows the easy identification of the alignment of each PTCDA molecule in the array. The period of the network is 34.6 Å, or $3\sqrt{3}a_0$, where $a_0 = 6.65$ Å is the lattice constant of the Ag−Si(111) $\sqrt{3} \times \sqrt{3}$R 30° surface. Both the period and the molecular orientations are the same as those observed by Theobald et al.[1,14] in previous studies of PTCDI−melamine networks.

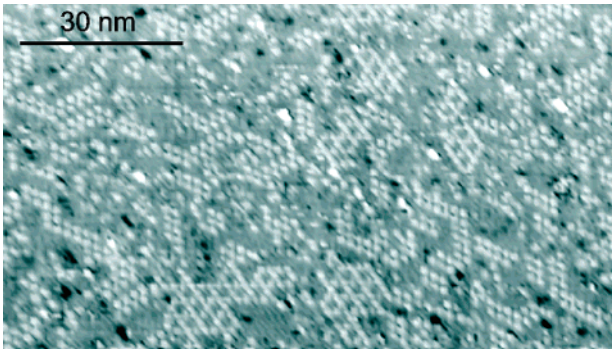

Figure 2. Overall surface morphology of PTCDA and melamine combined on the surface (sample bias −3 V, tunnel current 0.1 nA). The whole surface is covered by these hexagonal and double row structures.

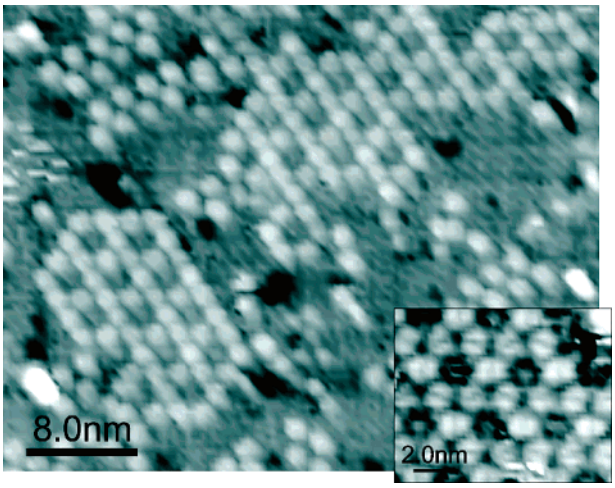

Figure 3. Image showing two regions of the PTCDA−melamine hexagonal network on the Ag−Si(111) $\sqrt{3} \times \sqrt{3}$R 30° surface. Areas of the double row phase can also be seen in the top left corner of the image. Insert: This high-resolution section of a hexagonal network shows the two halves of the HOMO of each PTCDA molecule (sample bias −3 V, tunnel current 0.1 nA for both images.)

A model is proposed for this molecular arrangement in Figure 4. The hexagonal background illustrated in the models is a schematic representation of the Ag−Si(111) $\sqrt{3} \times \sqrt{3}$R 30° surface. According to the widely accepted model for the atomic configuration of this surface (the honeycomb chain trimer model[15]), the vertexes correspond to the sites of silver trimers, and a silicon trimer is positioned at the center of each hexagonal repeat unit. The underlying silicon lattice vector $[1\bar{1}0]$ is indicated on all models as a reference direction.

In images of this phase, PTCDA molecules are visible, but melamine molecules cannot be readily resolved. From a comparison with our previous work we identify the vertexes of

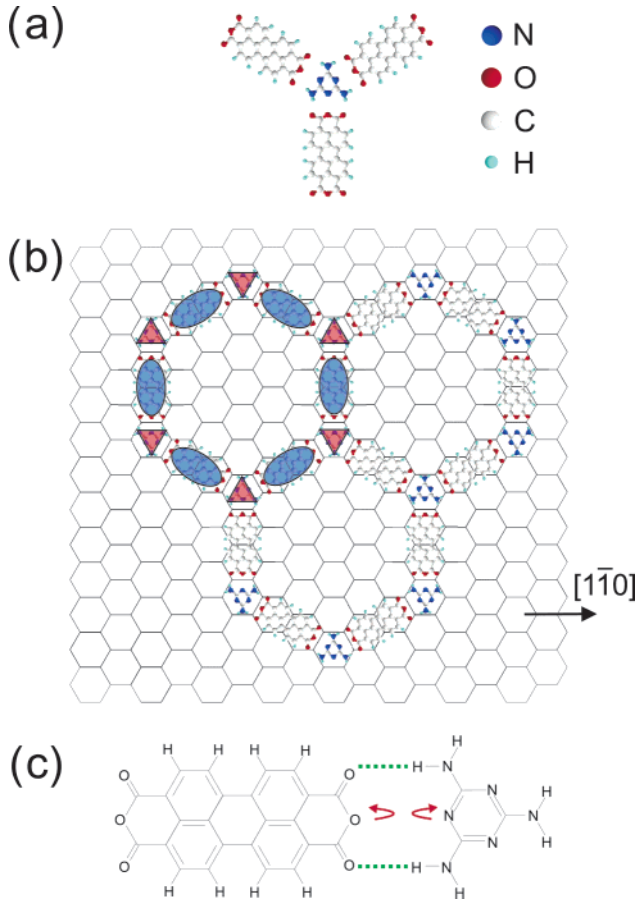

Figure 4. (a) Bonding junction present in the hexagonal phase. The key shows the colors of the different atoms present. (b) Model showing the molecules in the PTCDA−melamine network on the Ag−Si(111) $\sqrt{3} \times \sqrt{3}$R 30° surface. The ovals and triangles highlight the PTCDA and melamine molecules, respectively, in one hexagonal unit of the network. (c) The hexagonal network is stabilized partially by melamine molecules at the hexagon vertexes, hydrogen bonding via N−H···O interactions to the PTCDA anhydride groups, though there is an expected repulsion between the melamine ring nitrogen and the central dianhydride oxygen of PTCDA.

the network as melamine molecules.[1] Figure 4b shows a schematic of the molecular network on the Ag−Si(111) $\sqrt{3} \times \sqrt{3}$R 30° surface. As well as the stabilizing N−H···O bonds, there is also a potentially repulsive electrostatic interaction between the central anhydride oxygen atoms and the triazine ring nitrogen in the melamine, which both carry negative character (Figure 4c). The competition of energetics allows the phase to form; thus the possible repulsive interactions are overcome by the hydrogen bonds, which are strong enough to hold the network together. One may also consider the surface commensurability of this phase; from the model the molecules are all positioned in equivalent binding sites on the surface. To our knowledge no analogous molecular networks with equivalent hydrogen-bonded junctions have previously been observed in assembled structures or solution chemistry. This may not only reflect any instability of the anhydride/diaminopyridine interaction but also the observation that in solution anhydrides, including PTCDA, readily react with amines to afford imide moieties.[22]

It is therefore important to determine the stability of the network to confirm the validity of our proposed molecular model. Calculations performed on an arrangement of a single melamine molecule with three PTCDA molecules (Figure 5) indicate an interaction energy of −0.40 eV per 3-fold junction.

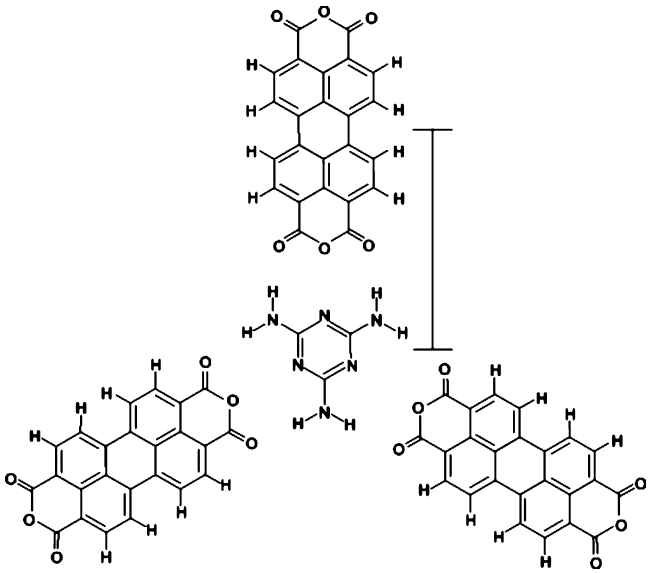

Figure 5. Diagram showing the calculated arrangement of a single junction of the hexagonal PTCDA−melamine arrangement. The distance between the center of the PTCDA and the melamine molecules (indicated) in the relaxed geometry is 10.3 Å

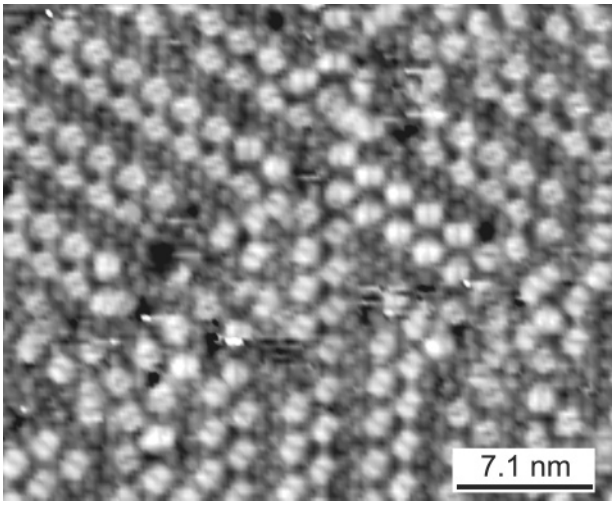

Figure 6. Image showing the molecules in the PTCDA−melamine double row phase on the Ag−Si(111) $\sqrt{3} \times \sqrt{3}$R 30° surface. Both molecular species can be resolved in this image (sample bias −3 V, tunnel current 0.1 nA).

This equates to an interaction energy of −0.13 eV per individual PTCDA−melamine junction, confirming that the proposed network is stabilized through weak but favorable interactions. The calculated spacing between the centers of PTCDA and melamine in the network is 10.3 Å, compared with the value proposed within our model (Figure 4) of $3a_0/2$, or 9.98 Å.

3.2. PTCDA and Melamine: Double Rows. As shown in Figure 3 another phase coexists with the hexagonal network. Figure 6 shows an STM image of this phase highlighting the presence of PTCDA−melamine double rows, which are the dominant motif observed in these studies. This phase consists of alternating double rows of PTCDA and melamine that lie along the ⟨11$\bar{2}$⟩ directions of the silicon lattice (indicated in Figure 7). The dimensions of the hexagonal network phase were used to determine molecular separations in the double row phase, as the underlying substrate could not always be resolved clearly in the images of the double rows. The spacing of adjacent PTCDA molecules in the direction parallel to the double rows was found to be $3a_0$. Similarly the separation of two PTCDA

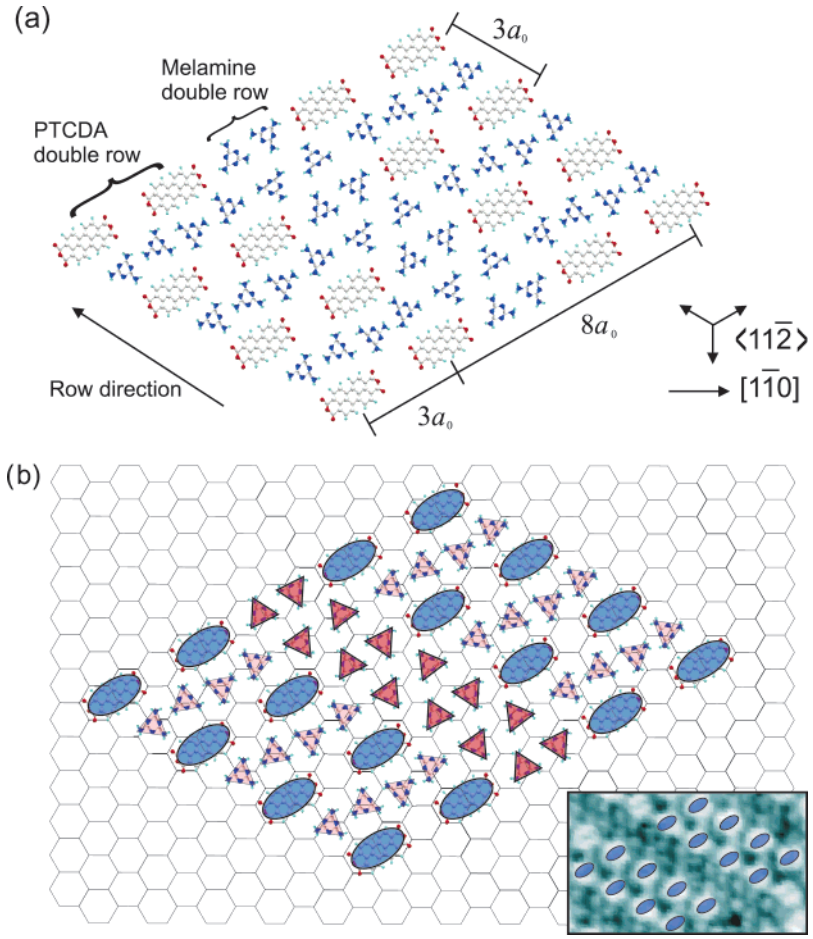

Figure 7. (a) Schematic model showing the molecular positions in the PTCDA−melamine double row structure. (b) A copy of part a including a lattice representing the underlying Ag−Si(111) $\sqrt{3} \times \sqrt{3}$R 30° surface. PTCDA molecules are highlighted with ovals, and melamine molecules are shown as triangles, shaded darker for the melamine double row, which is more easily resolved in the images. Insert: Section of image shown in Figure 6 with PTCDA molecules highlighted as in part b.

molecules across a double row, parallel to the molecular long axis, is $3a_0$. The distance between two adjacent double rows of PTCDA molecules was found to be $8a_0$. These dimensions, along with the observed orientations of the PTCDA molecules, allow us to accurately extract their relative positions on the surface (Figure 7). The angular orientation of the PTCDA molecules can be deduced from the direction of the HOMO lobes that run along the length of the molecule. Their separation and alignment are not consistent with close-packed PTCDA islands.[8]

Rows of melamine molecules form between the double rows of PTCDA molecules and may be clearly resolved in the STM images. There are two melamine molecules in each of the $3a_0$ repeat units separating PTCDA molecules in the direction parallel to the rows. Consequently every other melamine molecule is associated with an anhydride group. In the absence of defects, the melamine rows have a width corresponding to two molecules. At the junctions of rows we also observe small areas of melamine with a local hexagonal order. The fixed width of the rows suggests that there is a symmetry in the molecular packing that does not allow these structures to be extended in a regular fashion.

Pairs of PTCDA molecules within a double row are aligned end to end such that their anhydride groups point toward each other. Neighboring PTCDA molecules parallel to the row direction are too far apart (with a separation of $3a_0$) for a direct interaction between them to have a significant effect. Accordingly we propose a structure in which melamine molecules are coadsorbed between the PTCDA molecules stabilizing the double row arrangement. There is some evidence in the STM images of melamine molecules bound between PTCDA along the rows as bright, though not well defined, regions.

A model for molecular ordering is suggested in Figure 7. The positions and angular orientations of PTCDA molecules in this model have been accurately determined. It is important to note that the precise placement of melamine molecules within PTCDA double rows and the angular orientation of melamine molecules comprising double rows are approximate, since they are not well resolved in the images. Rather, melamine molecules in Figure 7 are positioned in such a way that might stabilize the PTCDA molecules through N−H···O interactions and may give rise to an axis of symmetry for the formation of PTCDA double rows only two molecules wide. It is not currently realistic to model this phase computationally due to the complexity of a single unit cell.

4. Conclusions

PTCDA and melamine have been found to form two intermixed phases when deposited on the Ag−Si(111) $\sqrt{3} \times \sqrt{3}$R 30° surface. We observe hexagonal networks and double row structures formed under the same growth conditions. The hexagonal networks are stabilized by an unexpected hydrogen bond where two N−H···O bonds flank a repulsive N−O interaction. This bonding junction has not previously been observed to our knowledge. Our results show that bonding

junctions that are not observed in other environments such as solution-based chemistry may be stable on a surface. Ab initio calculations confirm that the proposed bonding junction is stable. A second, more closely packed double row phase forms alongside the hexagonal network.

Acknowledgment. We acknowledge funding from the U. K. Engineering and Physical Sciences Research Council, Grant No. GR/S97521/01

References and Notes

(1) Theobald, J. A.; Oxtoby, N. S.; Phillips, M. A.; Champness, N. R.; Beton, P. H. *Nature* **2003**, *424*, 1029−1031.
(2) De Feyter, S.; De Schryver, F. C. *Chem. Soc. Rev.* **2003**, *32*, 139−150.
(3) Dmitriev, A.; Lin, N.; Weckesser, J.; Barth, J. V.; Kern, K. J. *Chem. Phys.* **2002**, *106*, 6907.
(4) Griessl, S.; Lackinger, M.; Edelwirth, M.; Hietschold, M.; Heckl, W. *Single Mol.* **2002**, *3*, 25−31.
(5) Barth, J. V.; Weckesser, J.; Trimarchi, G.; Vladimirova, M.; De Vita, A.; Cai, C.; Brune, H.; Günter, P.; Kern, K. *J. Am. Chem. Soc.* **2002**, *124*, 7991−8000.
(6) Weckesser, J.; De Vita, A.; Barth, J. V.; Cai, C.; Kern, K. *Phys. Rev. Lett.* **2001**, *87*, 096101.
(7) Keeling, D. L.; Oxtoby, N. S.; Wilson, C.; Humphry, M. J.; Champness, N. R.; Beton, P. H. *Nano Lett.* **2003**, *3*, 9−12.
(8) Swarbrick, J. C.; Ma, J.; Theobald, J. A.; Oxtoby, N. S.; O'Shea, J. N.; Champness, N. R.; Beton, P. H. *J. Phys. Chem. B* **2005**, *109*, 12167−12174.
(9) Whitesides, G. M.; Mathias, J. P.; Seto, C. T. *Science* **1991**, *254*, 1312−1319.
(10) Seto, C. T.; Whitesides, G. M. *J. Am. Chem. Soc.* **1993**, *115*, 905−916.
(11) Bobisch, C.; Wagner, T.; Bannani, A.; Möller, R. *J. Chem. Phys.* **2003**, *119*, 9804.
(12) de Wild, M.; Berner, S.; Suzuki, H.; Yanagi, H.; Schlettwein, D.; Ivan, S.; Baratoff, A.; Güntherodt, H.-J.; Jung, T. A. *ChemPhysChem* **2002**, *3*, 881−885.
(13) Bonifazi, D.; Spillmann, H.; Kiebele, A.; de Wild, M.; Seiler, P.; Cheng, F. Y.; Güntherodt, H.-J.; Jung, T. A.; Diederich, F. T. *Angew. Chem., Int. Ed.* **2004**, *43*, 4759−4763.
(14) Theobald, J. A.; Oxtoby, N. S.; Champness, N. R.; Beton, P. H.; Dennis, T. J. S. *Langmuir* **2005**, *21*, 2038−2041.
(15) Wan, K. J.; Lin, X. F.; Nogami, J. *Phys. Rev. B* **1993**, *47*, 13700−13723.
(16) Ordejón, P.; Artacho, E.; Soler, J. M. *Phys. Rev. B* **1996**, *53*, 10441−10444.
(17) Soler, J. M.; Artacho, E.; Gale, J.; Garcia, A.; Junquera, J.; Ordejón, P.; Sánchez-Portal, D. *J. Phys.: Condens. Matter* **2002**, *14*, 2745−2779.
(18) Becke, A. D. *Phys. Rev. A* **1988**, *38*, 3098−3100.
(19) Miehlich, B.; Savin, H.; Stoll, A.; Preuss, H. *Chem. Phys. Lett.* **1989**, *157*, 200−206.
(20) Troullier, N.; Martins, J. L. *Phys. Rev. B* **1991**, *43*, 1993−2006.
(21) Boys, S. B.; Bernadi, F. *Mol. Phys.* **1970**, *19*, 553.
(22) Würthner, F. *Chem. Commun.* **2004**, *14*, 1564−1579.